Accepted Manuscript

Title: CO oxidation over ceria supported Au_{22} nanoclusters: Shape effect of the support

Authors: Zili Wu, David R. Mullins, Lawrence F. Allard, Qianfan Zhang, Laisheng Wang

PII: S1001-8417(18)30050-0
DOI: https://doi.org/10.1016/j.cclet.2018.01.038
Reference: CCLET 4428

To appear in: *Chinese Chemical Letters*

Received date: 21-12-2017
Revised date: 11-1-2018
Accepted date: 19-1-2018

Please cite this article as: Zili Wu, David R.Mullins, Lawrence F.Allard, Qianfan Zhang, Laisheng Wang, CO oxidation over ceria supported Au22 nanoclusters: Shape effect of the support, Chinese Chemical Letters https://doi.org/10.1016/j.cclet.2018.01.038

Please donot adjust the margins

Communication

CO oxidation over ceria supported Au_{22} nanoclusters: Shape effect of the support

Zili Wu[a*], David R. Mullins[a], Lawrence F. Allard[b], Qianfan Zhang[c], Laisheng Wang[c]

[a]*Chemical Science Division and Center for Nanophase Materials Sciences, Oak Ridge National Laboratory, Oak Ridge, Tennessee 37831, USA.*

[b]*Materials Science and Technology Division, Oak Ridge National Laboratory, Oak Ridge, Tennessee 37831, USA.*

[c]*Department of Chemistry, Brown University, Providence, Rhode Island 02912, USA.*

Graphical Abstract

CO oxidation over ceria supported Au_{22} nanoclusters: Shape effect of the support

Zili Wu[a]*, David R. Mullins[a], Lawrence F. Allard[b], Qianfan Zhang[c], Laisheng Wang[c]

a. Chemical Science Division and Center for Nanophase Materials Sciences, Oak Ridge National Laboratory, Oak Ridge, Tennessee 37831, USA.

b. Materials Science and Technology Division, Oak Ridge National Laboratory, Oak Ridge, Tennessee 37831, USA.

c. Department of Chemistry, Brown University, Providence, Rhode Island 02912, USA.

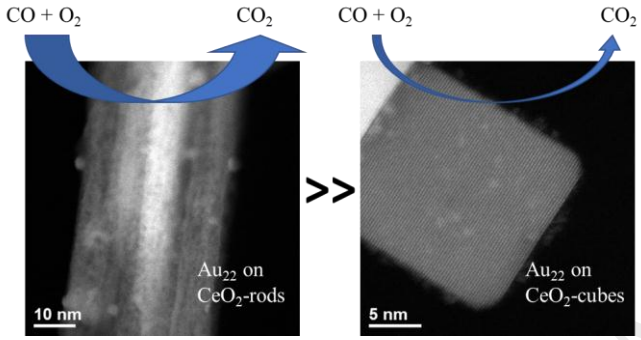

CO oxidation over ceria-supported Au_{22} nanoclusters shows strong dependence on the support shape: the lattice oxygen in CeO_2 rods is more reactive than in the cubes and thus make rods a superior support for Au nanoclusters in catalyzing low temperature CO oxidation

∗ Corresponding author.
E-mail address: wuz1@ornl.gov

Please donot adjust the margins

ARTICLE INFO

Article history:
Received 22 December 2017
Received in revised form 11 Jauary 2018
Accepted 12 January 2018
Available online

Keywords:
Gold nanoclusters
Ceria
Ligands
Support shape
CO Oxidation

ABSTRACT

Gold (Au) nanoclusters have recently emerged as ideal models for understanding Au catalysis, because the nanosized Au particles have precise atomic numbers and uniform size. In this work, we studied for the first time the support shape effect on the catalysis of Au nanoclusters by using CO oxidation as a model reaction. $Au_{22}(L^8)_6$ (L = 1,8-bis(diphenylphosphino) octane) nanoclusters were supported on CeO_2 rods or cubes, then pretreated at different temperatures (up to 673 K), allowing the gradual removal of the organic phosphine ligands. CO oxidation test over these differently pretreated samples shows that CeO_2 rods are much better supports than cubes for Au_{22} nanoclusters in enhancing the reaction rate. *In situ* IR spectroscopy coupled with CO adsorption indicates that the shape of CeO_2 support can impact the nature and quantity of exposed Au sites, as well as the efficiency of organic ligand removal. Although CeO_2 rods are helpful in exposing a greater percentage of total Au sites upon ligands removal, the percentage of active Au sites (denoted by $Au^{\delta+}$, $0 < \delta < 1$) is lower than that on CeO_2 cubes. The *in situ* extended X-ray absorption spectroscopy (EXAFS) and high-angle annular dark-field scanning transmission electron microscopy (HAADF-STEM) results show that the Au nanoclusters bound more strongly to the CeO_2 rods than to the cubes where the Au nanoclusters show more sintering. Considering the typical redox mechanism for CO oxidation over supported Au nanoclusters and nanoparticles, it is concluded that the reactivity of the lattice oxygen of CeO_2 is the determining factor for CO oxidation over Au_{22}/CeO_2. CeO_2 rods offer more reactive lattice oxygen and abundant oxygen vacancies than the cubes and thus make the rods a superior support for Au nanoclusters in catalyzing low temperature CO oxidation.

Supported gold nanocatalysts have attracted probably the most attention in recent decades in metal-support systems due to the intriguing particle size effect on the catalytic behaviors [1-5]. In revealing this effect in catalysis, tremendous efforts have been devoted to control the particle size and uniformity of Au nanoparticles among which ligand-protected Au nanoclusters clearly stand out as the ideal model system [3, 4, 6]. This is attributed to the atomic precision, uniform molecular size, and unique electronic and geometric structure of the Au nanoclusters [3, 4]. Au nanoclusters, supported or unsupported, have shown promising catalytic performances in hydrogenation, oxidation, and coupling reactions, offering precise analysis of the underlying reaction mechanism when the nanoclusters are kept intact [3, 6, 7].

Although the organic ligands can serve to maintain the atomic precision and uniform size of Au nanoclusters, they can also impact the catalysis of Au *via* electronic or geometric effects [3, 6]. It has been mostly accepted [8-15] that for gas phase reactions, the ligands play a negative role due to their geometric blockage of the active Au sites though a few studies [16-18] suggested otherwise. Removing the organic ligands generally opens up more Au sites and thus enhances the catalytic conversion or altered selectivity [8, 14]. During this ligand-stripping-off process, the coordination environment of Au nanoclusters switches from organic to inorganic ligands, *i.e.*, the support, introducing the so-called complex metal–support interaction [5, 19, 20]. Revealing the interaction between Au nanoclusters and the support is of significance for the understanding of Au catalysis through size-selected nanocluster model systems.

One of the approaches to the reveal the metal – support interaction is the use of shape-controlled supports as demonstrated for Au nanoparticles on nanoshaped oxides such as CeO_2, TiO_2 and Fe_2O_3 [20-23]. These nanoshaped oxides offer defined surface facets that simplify the factors contributing to the Au–support interaction. Currently, various supports including oxides and carbon have been used to anchor Au nanoclusters [8, 11, 14, 16, 24] and it has been shown that the nature of the support can play a big role in determining the activity of supported Au nanoclusters [11, 24]. However, the effect of support morphologies on the interaction with Au nanoclusters and the consequences for catalysis have not been studied. In this work, we make use of CeO_2 nanoshapes with defined surface facets [25], including rods and cubes, to support $Au_{22}(L^8)_6$ (L = 1,8-bis(diphenylphosphino) octane) nanoclusters. The removal of organic ligands, the evolution of Au surface sites upon interacting with CeO_2, and the reactivity in gas phase CO oxidation were carefully studied. We show that the surface facet of the CeO_2 support plays an important role in catalysis over Au nanoclusters via affecting the efficiency of the organic ligand removal, determining the nature and quantity of surface Au sites, and most importantly contributing reactive lattice oxygen for CO oxidation.

The synthesis of the two ceria nanoshapes has been described in detail in our recent work [25-28] while the $Au_{22}(L^8)_6$ (L = 1,8-bis(diphenylphosphino) octane) nanoclusters were synthesized using the method reported previously.[11, 29] For details, please refer to the supporting information. The successful synthesis of the free-standing $Au_{22}(L^8)_6$ nanoclusters was confirmed in our previous work *via* UV-vis-NIR absorption spectroscopy and electrospray ionization mass spectrometry (ESI-MS) [11, 29]. The CeO_2 rods and cubes supported $Au_{22}(L^8)_6$ nanoclusters are designated as Au_{22}/CeO_2-r and Au_{22}/CeO_2-c, respectively. The as-synthesized $Au_{22}(L^8)_6/CeO_2$ samples were characterized with high-angle annular dark-field scanning transmission electron microscopy (HAADF-STEM) and the images are shown in Fig.1 with different magnifications. These images clearly show that the $Au_{22}(L^8)_6$ nanoclusters are highly dispersed on both CeO_2 surfaces without obvious agglomeration. The Au nanoclusters show a uniform size of ~1.4 nm, consistent with what is expected from the theoretical value of the $Au_{22}(L^8)_6$ nanoclusters as our previous work [11] showed the nanoclusters are kept intact in the as-synthesized supported samples.

Please donot adjust the margins

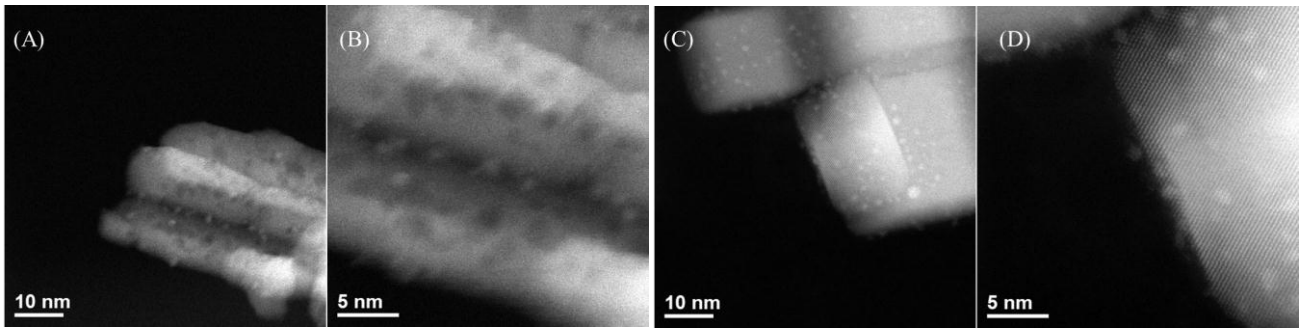

Fig. 1. HAADF-STEM images of as-synthesized $Au_{22}(L^8)_6$ /CeO_2-r (A) and (B) and $Au_{22}(L^8)_6$ /CeO_2-c (C) and (D) at different magnifications.

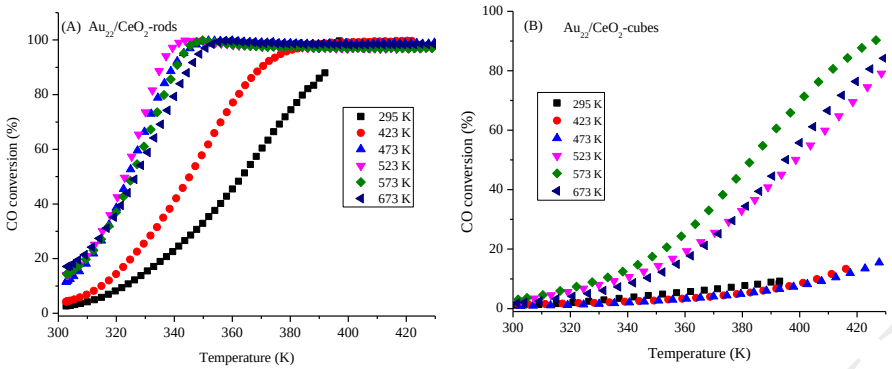

Fig. 2. CO oxidation light-off curves for different temperature pretreated (A) Au_{22} /CeO_2-r and (B) Au_{22} /CeO_2-c samples. O_2:CO = 2.5:1, space velocity: 28, 800 mL g^{-1} h^{-1}.

The different temperature pretreated Au_{22}/CeO_2 samples were tested for CO oxidation in the temperature range of 295–450 K and the CO oxidation light-off curves are shown in Fig.2. The samples pretreated at different temperatures were denoted as Au_{22}/CeO_2-r(c)-x where x represents the O_2-treatment temperatures. For example, Au_{22}/CeO_2-r-423 refers to $Au_{22}(L^8)_6/CeO_2$-r sample pretreated at 423 K in O_2 for 1 h. Similar to what has been demonstrated in our recent work for supported $Au_{22}(L^8)_6$ nanoclusters [11], the as-synthesized Au_{22}/CeO_2-r and Au_{22}/CeO_2-c samples already show activity at different levels for low temperature CO oxidation, again suggesting that the *in situ* coordination unsaturated (*cus*) Au sites in the Au_{22} nanoclusters are active for low temperature CO oxidation. The support morphology of the CeO_2 results in a drastic difference in CO oxidation activity: the as-synthesized Au_{22}/CeO_2-r shows >80% conversion at 380 K while the as-synthesized Au_{22}/CeO_2-c converts less than 20% CO at the same temperature. Upon high temperature pretreatments, the support shape effect is also evident on the activity of Au_{22} nanoclusters for CO oxidation. For Au_{22}/CeO_2-r, the activity in CO oxidation keeps increasing as the pretreatment temperature is elevated, due to the removal of the phosphine ligands and the introduction of Au–CeO_2 interaction.[11] 100% conversion is obtained at a temperature below 350 K for the Au_{22}/CeO_2-r samples pretreated at 473 K and above. A slight decrease in the reactivity is observed after 673 K pretreatment in comparison to Au_{22}/CeO_2-r treated at 573 K. For Au_{22}/CeO_2-c, pretreatment at 423 K and 473 K resulted in activity similar to the as-synthesized sample. A dramatic increase in CO oxidation activity is observed for samples pretreated at 523 K and above. The 573 K-pretreated sample gives the highest conversion and the 673 K-pretreated one shows some decrease in CO conversion. 100% conversion of CO was not achieved on the Au_{22}/CeO_2-c samples in the tested temperature range up to 430 K.

Apparently, CeO_2 rods are much better supports for the de-ligated Au_{22} nanoclusters than the cubes. The T_{50}, or the temperature at which CO conversion is 50%, for the Au_{22}/CeO_2-r and Au_{22}/CeO_2-c samples is compared in Table S1 (Supporting information) and has often been used for comparison of different catalysts for low temperature CO oxidation [30]. The T_{50} for the Au_{22}/CeO_2-r samples is almost 60 K lower than Au_{22}/CeO_2-c, indicating higher reactivity of the Au nanoclusters on CeO_2 rods. As shown below (EXAFS and STEM study of Au nanoclusters), the organic ligands are completely removed from the Au_{22} nanoclusters after 573 K pretreatment and thus the Au nanoclusters interact completely with the ceria support after this temperature treatment. So we compare the turnover frequency (TOF) for CO oxidation over the samples at CO conversion less than 20% at differential condition. At a reaction temperature of 310 K, the TOF is 0.023 and 0.007 s^{-1} for Au_{22}/CeO_2-r-573 and Au_{22}/CeO_2-c-573, respectively. CeO_2 rods-supported Au nanoclusters are about 3 times more reactive than those supported on the cubes. These TOFs are on par with those obtained for Au_{22} nanoclusters supported on TiO_2 [11] and other supported Au nanoparticles [31, 32], The TOF was calculated based on the number of surface Au sites, which was estimated from the size (d) of the Au particles after 573 K-pretreatment using 1/d as the dispersion. As shown in the following STEM 573 and Au_{22}/CeO_2-c-573 are 1-1.5 nm and 1.5–2 nm, respectively. An average of 1.3 nm and 1.8 nm was used for the calculation of the surface Au sites of Au_{22}/CeO_2-r-573 and Au_{22}/CeO_2-c-573, respectively.

Please donot adjust the margins

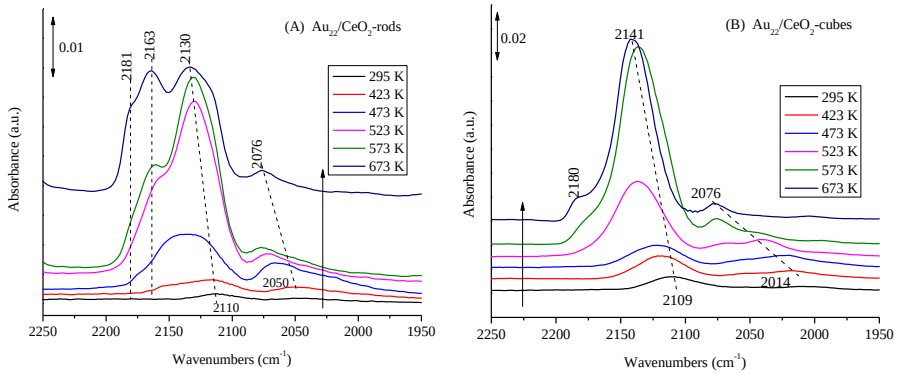

Fig. 3. IR spectra of CO adsorption at room temperature on (A) Au_{22} /CeO_2-r and (B) Au_{22} /CeO_2-c samples pretreated in O_2 at different temperatures.

The significant support shape effect is investigated in the following sections *via in situ* IR spectroscopy to probe the nature of surface Au sites, and *in situ* EXAFS and STEM to probe the coordination environment and size evolution of the Au nanoclusters.

IR spectra from CO adsorption on the Au_{22}/CeO_2 samples after pretreatment at different temperatures are shown in Fig.3. For the two as-synthesized samples, a weak band at ~2100 cm^{-1} is observed and can be ascribed to CO adsorbed on metallic Au sites [33-35] , *i.e.*, the *cus* Au sites within the intact Au_{22} nanoclusters. In general, with the increase of pretreatment temperatures of the Au_{22}/CeO_2 samples, the IR bands from adsorbed CO increase in intensity and simultaneously shift from 2107 cm^{-1} on the as-synthesized samples to higher wavenumbers. These changes are due to the gradual removal of the phosphine ligands and the increased Au – CeO_2 interaction [8, 11]. But the Au_{22}/CeO_2-r and Au_{22}/CeO_2-c samples show some differences in the spectral evolution. For the Au_{22}/CeO_2-r samples (Fig.3A), a slight increase in the intensity of the CO bands is observed for the sample treated < 423 K or > 523 K, while a considerable increase is observed for those treated between 423 K and 523 K. For the Au_{22}/CeO_2-c samples (Fig.3B), a significant increase in the intensity of the bands is seen for samples treated between 473 K and 573 K, while insignificant change is observed for treatment < 473 K and > 573 K. Three types of Au sites are probed from CO adsorption on the samples pretreated at 573 K and above: 2163 cm^{-1} due to CO-Au^+, 2130 cm^{-1} due to CO-$Au^{\delta+}$ ($0 < \delta < 1$) and 2076 cm^{-1} due to CO-$Au^{\delta-}$ [8, 11]. The band at 2181 cm^{-1} is due to CO adsorption on *cus* Ce cations sites.[8] The majority Au sites, $Au^{\delta+}$, are the active centers for low temperature CO oxidation as demonstrated in our previous work on Au nanoclusters.[8, 11] For the Au_{22}/CeO_2-c sample (Fig.3B), pretreatment at 423 and 473 K results in a slight increase in CO band intensity. 523 K pretreatment leads to a moderate increase in CO bands with the strongest increase for the 573 K pretreated sample. Two types of Au sites are revealed by CO adsorption on high temperature pretreated Au_{22}/CeO_2-c samples: 2141 cm^{-1} due to CO-$Au^{\delta+}$ ($0 < \delta < 1$) and 2076 cm^{-1} due to CO-$Au^{\delta-}$. The lack of Au^+ sites on CeO_2 cubes as compared to rods implies a support shape effect in determining the type of surface Au sites in the Au nanoclusters.

For both Au_{22}/CeO_2 samples, 573 K pretreatment leads to the largest amount of exposed Au sites as demonstrated by the integrated area of the CO bands. The Au site exposures for the different temperature pretreated samples were obtained by integrating the CO bands and taking the ratio to that of the 573 K sample. Even though our previous work on Au_{25}/CeO_2-rods and Au/SiO_2 [8, 33] showed that the IR absorption coefficient for CO on metallic Au is larger than on cationic Au (no more than 50%), we did not consider the influence of the absorption coefficient difference on the IR intensity for CO adsorbed on differently treated Au_{22}/CeO_2 because majority of the Au sites is cationic. The result is shown in Fig.S1 (Supporting information). A clear difference is the exposure of Au sites after moderate temperature pretreatment for Au_{22}/CeO_2-r and Au_{22}/CeO_2-c samples: much less exposure of Au sites for CeO_2 cube-supported Au nanoclusters after 473 K and 523 K pretreatment, indicating more difficult removal of the phosphine ligands on the Au_{22} nanoclusters when supported on CeO_2 cubes than on the rods. It appears that the removal of the ligands is facilitated by the higher reactivity of lattice oxygen in CeO_2 rods than in cubes [28].

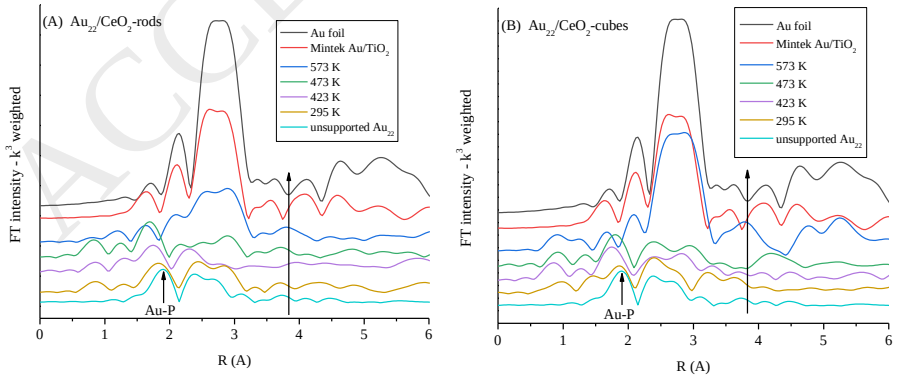

Fig. 4. EXAFS spectra of (A) Au_{22} /CeO_2-r and (B) Au_{22} /CeO_2-c samples pretreated at different temperatures in O_2. Spectra from unsupported $Au_{22}(L^8)_6$, Au foil and Mintek Au/TiO_2 catalyst are also shown as references.

The state of the phosphine ligands and the size of the supported Au_{22}/CeO_2 were followed by *in situ* EXAFS after pretreatment at different temperatures and the spectra are shown in Fig. 4. The spectra from an unsupported $Au_{22}(L^8)_6$ nanocluster sample, the Mintek Au/TiO_2 standard and gold foil are also shown for comparison. The Au-P single scattering peak has an apparent, non-phase-shift corrected position at 1.91 Å for the unsupported Au_{22} nanoclusters. The Au-P coordination number (CN) was determined to be 0.5 which is in excellent agreement with actual value of 0.55. The Au-P peak appears to shift slightly to a shorter distance when the $Au_{22}(L^8)_6$ is supported on both CeO_2 nanoshapes, possibly due to the interaction of the nanoclusters with the CeO_2 support. The fit to the data indicated that both the Au-P distance and CN are unchanged. The structure of the Au_{22} core in the as-synthesized $Au_{22}(L^8)_6/TiO_2$ also largely resembles that of the unsupported nanoclusters as evident from the similar features of the Au-Au peaks in the 2~3 Å range. These observations suggest that the Au_{22} nanoclusters dispersed on the two different shapes of CeO_2 surfaces are similarly coordinated with the diphosphine ligands as in the unsupported case and are structurally intact. This confirms that the *in situ cus* Au sites in the as-synthesized Au_{22}/CeO_2 samples are responsible for the low temperature CO oxidation (Fig.2).

When the Au_{22}/CeO_2 samples were treated in O_2 at higher temperatures, the Au-P and Au-Au peaks in the EXAFS spectra do not show significant changes in intensity up to 473 K, implying minimal change in the coordination situation of the Au_{22} nanoclusters on both CeO_2 rods and cubes. The position and contour of the peaks in these two regions show some variations in these samples, possibly a result of the structural rearrangement of the Au nanoclusters on the CeO_2 supports upon thermal treatment. After 573 K treatment, the Au-P peak disappears for both samples, indicating the complete removal of the phosphine ligands at this temperature. At the same time, the Au-Au peak increases in intensity with more of an increase for the Au_{22}/CeO_2-c-573 (Fig.4B) sample than Au_{22}/CeO_2-r-573 (Fig.4A). The increase is a sign of greater Au-Au coordination and thus particle growth. The growth of Au nanoclusters at 573 K is likely associated with the removal of the diphosphine ligands at this temperature, which is consistent with previous observations for Au_{22} on a TiO_2 surface and the TGA results [11]. The coordination number for Au from fitting for the Au_{22}/CeO_2-c-573 and Au_{22}/CeO_2-r-573 samples are 8.6 and 6.8, corresponding to particle size of 1.5-2 nm and 1–1.5 nm, respectively [36]. The Au-Au coordination for the Mintek Au/TiO_2 standard is fitted as 9.2, corresponding to Au particle size of 2–2.5 nm, slightly smaller than the average size of 3.2 nm as determined by TEM [37].

The size evolution of the Au nanoclusters was also visually followed by the dark-field HAADF-STEM imaging after the two Au_{22}/CeO_2 samples were treated at 423, 473 and 573 K (Fig.S2 in Supporting information). The size of the Au nanoclusters does not show obvious change after 423 and 473 K treatment as compared to those of the as-synthesized nanoclusters (Fig.1), consistent with the EXAFS result. The growth of Au nanoclusters is observed for both Au_{22}/CeO_2 samples after 573 K treatment, with more growth on the Au_{22}/CeO_2-c-573 sample, also in good agreement with the EXAFS data. Although the size of Au nanoclusters appears larger than what was estimated from the EXAFS result, the trend of Au particle size is consistent: Mintek Au/TiO_2 > Au_{22}/CeO_2-c-573 > Au_{22}/CeO_2-r-573. It is evident that the Au nanoclusters are better stabilized by ceria rods than cubes. This is similar to what has been observed for Au nanoparticles when supported on ceria rods and cubes: better stabilization of Au nanoparticles on rods than on cubes, which was attributed to the strong interfacial interaction between Au particles and rods' surface [20, 21, 38].

The catalytic consequence of the CeO_2 shape effect on Au_{22} nanoclusters is that the CO oxidation activity is always much lower on Au_{22}/CeO_2-c than Au_{22}/CeO_2-r after the same pretreatment temperature (Fig.2). Several other consequences from the support shape effect were also observed: a) the nature of exposed Au sites upon thermal treatment is different for Au_{22} nanoclusters supported on CeO_2 rods vs cubes. There are more positively charged Au sites, i.e., Au^+, on CeO_2 rods than cubes after the complete removal of the phosphine ligands (IR results in Fig.3); b) the removal of phosphine ligands in the Au_{22} nanoclusters is more facile on the CeO_2 rods than on cubes (IR results in Fig.3); c) the interaction between Au nanoclusters and CeO_2 support is stronger on rods than on cubes as evidenced by the smaller Au size after treatment at 573 K (EXAFS and STEM in Figs. 4 and 5). To explain the catalytic consequence of support shape effect, one needs to consider the reaction mechanism of CO oxidation over supported Au nanoclusters. Our previous work [8, 11] clearly suggests that a redox mechanism dominates the CO oxidation pathways over Au nanoclusters supported on reducible oxides such as CeO_2 and TiO_2, where the lattice oxygen of the support oxidizes CO adsorbed on the Au sites to CO_2. Therefore, the reactivity of supported Au nanoclusters depends on the activation and reactivity of both CO (on the Au sites) and oxygen (on the oxide support), which is impacted by the shape of the CeO_2 support from our current work along with previous studies. The contribution from CO on Au sites and O on the oxide support are discussed in detail below:

Activation and reactivity of CO: It is known that both the quantity and nature of exposed Au sites are important in determining the reactivity of adsorbed CO. For Au_{22}/CeO_2-r, the higher CO oxidation activity after moderate temperature pretreatment (473–523 K) can be partially attributed to the more available Au sites exposed after facile removal of phosphine ligands than the Au_{22}/CeO_2-c sample. After the complete ligand removal at a temperature of 573 K and above, both the amount and nature of exposed Au sites are different on CeO_2 rods and cubes. The smaller size of Au nanoclusters on CeO_2 rods than on cubes affords more surface Au sites (by ~20% from as the EXAFS-estimated average Au size). However, this effect is countered by a smaller percentage of active Au sites ($Au^0 + Au^{\delta+}$ ($0 < \delta < 1$)) on Au_{22}/CeO_2-r as shown in Fig.3. For supported Au nanoclusters,[8, 11] it was shown that metallic Au and cationic $Au^{\delta+}$ ($0 < \delta < 1$) are active for low temperature CO oxidation while negatively charged Au and Au^+ are only active at higher temperatures. After pretreatment at 573 K and 673 K, the Au_{22}/CeO_2-r sample possesses about 60% (from peak fitting of the IR spectra) $Au^{\delta+}$ ($0 < \delta < 1$), less than the ~85% of active Au sites in Au_{22}/CeO_2-c. However, the reactivity of Au nanoclusters on CeO_2 rods is much higher (3~4 times) for CO oxidation than on cubes. Therefore, it appears that the difference in the amount of active Au sites (~20%) is far from compensating the large difference in the catalytic activity of the two types of catalysts. The reactivity of the lattice oxygen of the different CeO_2 nanoshapes must be accounted for.

Activation and reactivity of O: It has been demonstrated that CO oxidation proceeds predominantly via a redox mechanism on both CeO_2 and Au/CeO_2 catalysts [8, 11, 28, 38]. Therefore, the reactivity of the lattice oxygen largely determines the activity for CO

oxidation. Through temperature programmed reduction (TPR) with CO and oxygen isotope exchange experiments [28], the lattice oxygen in CeO_2 rods was found to be much more reactive and mobile than in cubes. This was attributed to the lower oxygen vacancy formation energy for (110) facets and larger number of defects in rods than in cubes (terminated with (100) facets) [25, 28]. When Au_{22} nanoclusters are supported on CeO_2, the active Au sites are in close proximity to the oxide surface[11] regardless of the presence of phosphine ligands. Therefore, it is anticipated that more reactive lattice oxygen in CeO_2 rods will result in higher reactivity to oxidize the CO molecules adsorbed on the Au sites than the cubes.

In summary, the shape effect of the ceria support on the catalytic CO oxidation by Au_{22} nanoclusters has been studied in this work. CeO_2 rod-supported Au nanoclusters are always several times more active for low temperature CO oxidation than cube-supported nanoclusters at different stages of organic ligand removal. The support effect was investigated through a combination of techniques including *in situ* IR spectroscopy, EXAFS and STEM. It was shown that during the de-ligation process, the shape of the CeO_2 support controls a) the nature and amount of exposed Au sites; b) the ease of organic ligand removal; and c) the interaction strength between Au and CeO_2 and thus the particle size of Au. The smaller Au particles and the easier removal of organic ligands for Au nanoclusters supported on CeO_2 rods is part of the reason for observing better CO oxidation activity than on CeO_2 cubes. But the major support shape effect is found to be the different reactivity of the lattice oxygen of the CeO_2 nanoshapes where the rods offer highly reactive lattice oxygen to oxidize adsorbed CO on the Au sites to produce CO_2. This work provides a fundamental understanding of support shape in Au nanocluster catalysis and points to a design strategy of more active Au nanocluster catalysts by using shape-controlled oxide supports.

Acknowledgment

The work was supported by the U.S. Department of Energy, Office of Science, Basic Energy Sciences, Chemical Sciences, Geosciences, and Biosciences Division. Part of the work including the IR study was conducted at the Center for Nanophase Materials Sciences, which is a DOE Office of Science User Facility. Use of the Stanford Synchrotron Radiation Lightsource, SLAC National Accelerator Laboratory, is supported by the U.S. Department of Energy, Office of Science, Office of Basic Energy, Sciences under Contract No. DE-AC02-76SF00515. We acknowledge the facilities support at the beamline BL 2-2 provided by the Synchrotron Catalysis Consortium U.S. DOE (No. De-SC0012335).

References

[1] M. Valden, X. Lai, D.W. Goodman, Science 281 (1998) 1647-1650.
[2] A.S.K. Hashmi, G.J. Hutchings, Angew. Chem. Int. Ed. 45 (2006) 7896-7936.
[3] G. Li, R.C. Jin, Acc. Chem. Res. 46 (2013) 1749-1758.
[4] R. Jin, C. Zeng, M. Zhou, Y. Chen, Chem. Rev. 116 (2016) 10346-10413.
[5] M. Haruta, Catal. Today 36 (1997) 153-166.
[6] C. Zeng, Y. Chen, S. Zhao, R. Jin, Chapter 10 - Atomically Precise Gold and Bimetal Nanoclusters as New Model Catalysts, in: P. Fornasiero, M. Cargnello (Eds.) Studies in Surface Science and Catalysis, Elsevier, Amsterdam, 2017, pp. 359-408.
[7] Y. Chen, R. Jin, Chapter 10 - Atomically Precise Gold Nanoclusters Catalyzed Chemical Transformations, in: T. Tatsuya, H. Hannu (Eds.) Frontiers of Nanoscience, Elsevier, Amsterdam, 2015, pp. 263-296.
[8] Z.L. Wu, D.E. Jiang, A.K.P. Mann, et al., J. Am. Chem. Soc. 136 (2014) 6111-6122.
[9] G.C. Ma, A. Binder, M.F. Chi, et al., Chem. Commun. 48 (2012) 11413-11415.
[10] S. Gaur, J.T. Miller, D. Stellwagen, et al., Phys. Chem. Chem. Phys. 14 (2012) 1627-1634.
[11] Z. Wu, G. Hu, D.E. Jiang, et al., Nano Letters 16 (2016) 6560-6567.
[12] B. Zhang, S. Kaziz, H. Li, et al., J. Phys. Chem. C 119 (2015) 11193-11199.
[13] J. Fang, J. Li, B. Zhang, et al., Nanoscale 7 (2015) 6325-6333.
[14] T. Yoskamtorn, S. Yamazoe, R. Takahata, et al., ACS Catal. 4 (2014) 3696-3700.
[15] L.D. Menard, F.T. Xu, R.G. Nuzzo, J.C. Yang, J. Catal. 243 (2006) 64-73.
[16] J. Good, P.N. Duchesne, P. Zhang, et al., Catal. Today 280 (2017) 239-245.
[17] W. Li, Q. Ge, X. Ma, et al., Nanoscale 8 (2016) 2378-2385.
[18] X.T. Nie, H.F. Qian, Q.J. Ge, et al., ACS Nano 6 (2012) 6014-6022.
[19] G.L. Haller, D.E. Resasco, Metal–Support Interaction: Group VIII Metals and Reducible Oxides, in: D.D. Eley, H. Pines, P.B. Weisz (Eds.) Advances in Catalysis, Academic Press, Cambridge, 1989, pp. 173-235.
[20] Y. Lin, Z. Wu, J. Wen, et al., Nano Lett. 15 (2015) 5375-5381.
[21] R. Si, M. Flytzani-Stephanopoulos, Angew. Chem. Int. Ed. 47 (2008) 2884-2887.
[22] Y. Li, W. Shen, Chem. Soc. Rev. 43 (2014) 1543-1574.
[23] Z.-A. Qiao, Z. Wu, S. Dai, ChemSusChem 6 (2013) 1821-1833.
[24] G. Li, D.E. Jiang, C. Liu, et al., J. Catal. 306 (2013) 177-183.
[25] Z. Wu, M. Li, J. Howe, et al., Langmuir 26 (2010) 16595-16606.
[26] A.K.P. Mann, Z. Wu, F.C. Calaza, S.H. Overbury, ACS Catal. 4 (2014) 2437-2448.
[27] Z. Wu, A.K.P. Mann, M. Li, S.H. Overbury, J. Phys. Chem. C 119 (2015) 7340-7350.
[28] Z. Wu, M. Li, S.H. Overbury, J. Catal. 285 (2012) 61-73.
[29] J. Chen, Q.F. Zhang, T.A. Bonaccorso, et al., J. Am. Chem. Soc. 136 (2014) 92-95.
[30] Z. Ma, S. Dai, ACS Catal. 1 (2011) 805-818.
[31] W. Yan, B. Chen, S.M. Mahurin, et al., J. Phys. Chem. B 109 (2005) 10676-10685.
[32] M. Li, Z. Wu, S.H. Overbury, J. Catal., 278 (2011) 133-142.
[33] Z.L. Wu, S.H. Zhou, H.G. Zhu, et al., J. Phys. Chem. C 113 (2009) 3726-3734.

Please donot adjust the margins

[34] Z.L. Wu, S.H. Zhou, H.G. Zhu, et al., Chem. Commun. (2008) 3308-3310.
[35] A. Chiorino, M. Manzoli, F. Menegazzo, et al., J. Catal. 262 (2009) 169-176.
[36] A.I. Frenkel, C.W. Hills, R.G. Nuzzo, J. Phys. Chem. B 105 (2001) 12689-12703.
[37] C.G. Long, J.D. Gilbertson, G. Vijayaraghavan, et al., J. Am. Chem. Soc. 130 (2008) 10103-10115.
[38] N. Ta, J. Liu, S. Chenna, et al., J. Am. Chem. Soc. 134 (2012) 20585-20588.